

NEWS ON ESO INSTRUMENTATION

Status Report on EMMI: Results from the Testing in Garching

H. DEKKER and P. MOLARO, ESO

In the *Messenger* No. 57 of September 1989 a status report on EMMI was given at the start of the integration and test period. This period has now been concluded; at the time these lines are written the instrument is about to be packed and shipped to La Silla. The integration of the instrument in the NTT Nasmyth room B will take place this spring. Installation at the telescope will take place as soon as the second adaptor/rotator of the NTT is fully tested at the end of June and a first period of tests on the adapter is scheduled for July. We describe here some of the results obtained during the tests in Garching.

The image quality is a complex function of focus, position on the CCD and wavelength (because of secondary colour in the lens optics) so it is difficult to give a single number. In general, image quality in the red arm is at the level of 10–25 μm . EMMI was tested and will be initially used with the red F/2.5 camera and 1024 \times 1024 Thomson 3156 chip. The blue optics are now in the last phase of assembly at the manufacturer. We intend to fit the blue F/4 camera and a coated Thomson chip during the integration on La Silla. With these cameras, the pixel matching will be 0.45 (red) and 0.28 arcsec/pixel (blue). The experience with EFOSC2 (matching .15–.25 arcsec/pixel, depending on the detector mounted) has shown that image sampling at this scale is necessary if we are to exploit the not-too-rare periods of excellent seeing at the NTT. For direct imaging in the red we are considering the option of a second long camera. For instance, the F/5.3 camera combined with a Tektronix 1024 \times 1024 chip with 24 μm pixels will provide a matching of 0.27 arcsec/pixel and a field of 4.5 \times 4.5 arcmin at the expense of reduced wavelength coverage in grism spectroscopy. Another possibility would be a 2048 \times 2048 Ford CCD with 15 micron pixels. The decision for a high resolution red camera/CCD option will be taken later this year depending on a number of mainly operational considerations.

EMMI being a multipurpose instrument, the light meets more optical surfaces than would be necessary in a dedicated instrument. This was one of the reasons for splitting the instrument in

two channels in order to enable the use of optimized multilayer coatings. As an example of what can be obtained with

these coatings, the on-axis transmission of the red medium dispersion collimator is shown in Figure 1. From measure-

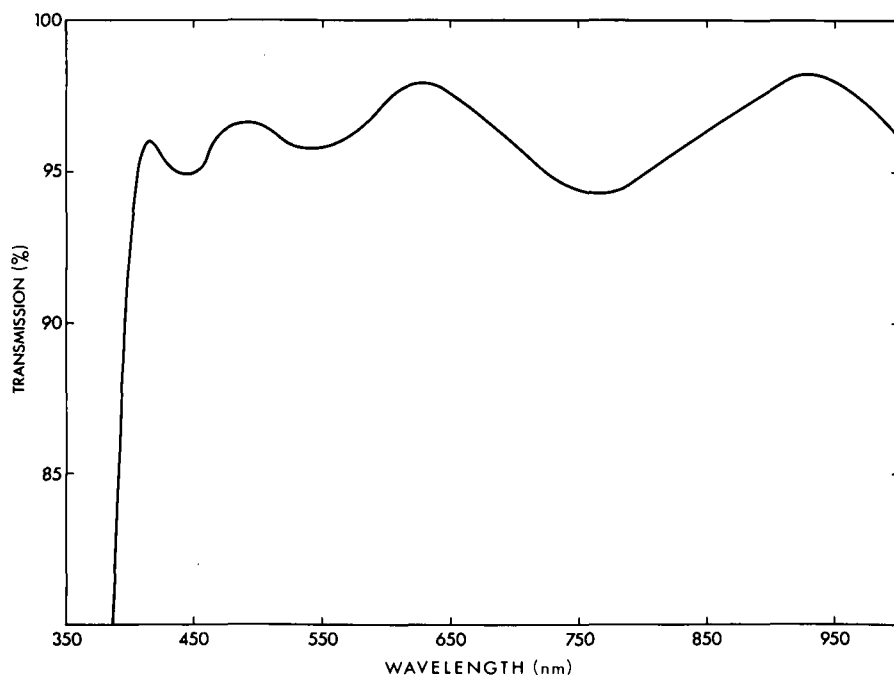


Figure 1: The transmission of the red collimator (consisting of two cemented doublets) in single pass. It is used in double pass, so the total efficiency in the range 4000–10000 \AA will be over 90%, still better than a single aluminium mirror.

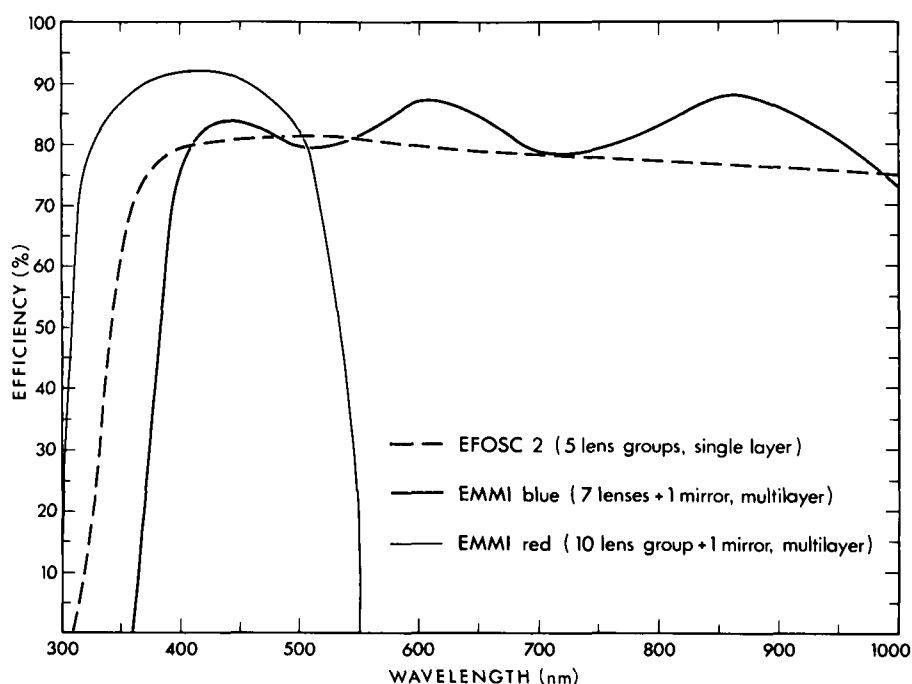


Figure 2: The efficiency of the EMMI optics in imaging and low dispersion as compared with EFOSC2.

ments of the optical units we calculate an overall efficiency of 85 and 70% in the red imaging/low dispersion and medium dispersion modes respectively; somewhat better in the corresponding blue modes. EMMI is in each of these modes more efficient than the competing 3.6-m instruments EFOSC, Boller & Chivens or Caspec. Figure 2 compares the efficiency of EMMI in imaging and low dispersion with EFOSC2.

Ghosts and stray light are very low. Lens optics in spectrographs have a well-known disadvantage which is the possibility of spurious reflections. With modern optical design programmes such ghosts can be accurately predicted and – by adjusting the design parameters – reduced to insignificant levels. In fact, the only noticeable ghost occurs at a cemented interface in the collimator which has a reflectivity of .01% and had not been considered in the ghost analysis.

EMMI will be mounted at the adapter of the NTT and is co-rotating to follow the field rotation. Rotation rates when tracking near the zenith will be much higher than the 15 deg/hour experienced by instruments at equatorial telescopes. Our design specification for flexure calls for an image motion on the detector of less than 10 μm in the dispersion direction when rotating the instrument by 180 degrees, a very hard requirement in view of the large number of moving functions and the size of EMMI. A typical assignment within the image motion error budget calls for a contribution of 2 μm due to any particular function. For the grating unit this translates into a maximum admissible flexure of just 0.4 arcsec on the grating surface when turning the unit upside down! The structure of EMMI, the grating units as well as many other critical units were each individually tested and many improvements were made in order to meet this objective. Further flexure tests of the complete instrument will be carried out at the telescope.

EMMI was controlled by an engineering version of the control software which was continuously improved during the test period. A first version of the user interface with softkeys and forms on the Ramtek monitor was also tested. We used a Thomson 1024 \times 1024 setup chip mounted on the red arm, controlled by the new VME camera and a stand-alone version of the new CCD programme, a configuration sufficient for the Garching tests. All in all, the integration and test of EMMI in Garching proceeded very smoothly and without major negative surprises. Still, a substantial amount of work remains to be done for



Figure 3: The echelle spectrum of a nearby G-type star taken with EMMI from Garching. Note the strong O_2 bands in orders 20 and 23 caused by the large airmass and low altitude.

the integration of the EMMI hard- and software with the NTT environment.

As an appetizer for future users, we show in Figure 3 an echelle spectrum of the Sun (probably the first solar spectrum ever recorded from Garching) taken with a 3-cm telescope and a 35-m fiber link. This sun spectrum gives a first impression of the quality of the data that can be obtained with this instrument. Note that echelle spectroscopy is a demanding application; focus and image quality must be optimized in a large wavelength range over the complete CCD field and stray light and ghosts are most apparent in echelle mode.

The spectrum has been recorded using a slit with a width of 0.5 arcsec and a height of about 17 arcsec (38 pixels) that was illuminated along its full height by diffused sunlight from the fiber. A star spectrum would appear much narrower depending on the seeing and tracking accuracy. In the figure, red (up to 7700 \AA) is at the top and blue (starting at 4000 \AA) at the bottom. The figure does not dis-

play the whole CCD because the image has been truncated to eliminate two dead columns on the right side of the setup chip. However, this does not cause any spectral gap since the adjacent orders overlap for about 90 \AA each side. Expert eyes can recognize at a glance the atmospheric A and B O_2 bands in orders 20 and 23 (the first and the fourth order counting from the top), H_α at the centre of order 24, the D_1 and D_2 resonance lines of NaI on order 27, the MgIb multiplet at $\lambda\lambda \approx 5170 \text{\AA}$ in order 31 and H_β in order 33.

Figure 4 displays a portion of the extracted and wavelength calibrated order 24. Background has been evaluated averaging from the two adjacent inter-orders and subtracted. The calibration in wavelength has been performed using an image of a Thorium/Argon lamp taken with the same set-up. Then the order has been normalized with a spline interpolation through continuum windows. To check the photometric accuracy we have measured the equivalent

widths of the strongest lines, not contaminated by water-vapour lines. The comparison of our equivalent widths with those of the Moore et al. (1966) solar atlas, paying attention to add all the possible contributions, has shown an agreement within $\pm 0.004 \text{ \AA}$, and without systematic trends. Such a small difference can be easily accounted for considering the uncertainty in the drawing of the continuum and the accuracy of the measurements in our spectrum that has a S/N of ≈ 200 .

The level of the scattered light measured in the interorder region stays fairly low all over the CCD and in the red it remains below 2% of the nearby order intensity.

The spectral resolution measured from the arc image is slightly varying from one order to the other likely due to non-perfect focusing over the entire wavelength range. The best resolution is found in order 28 where the average FWHM of the arc lines is 0.48 \AA giving a resolving power of $\approx 12,000$. This is

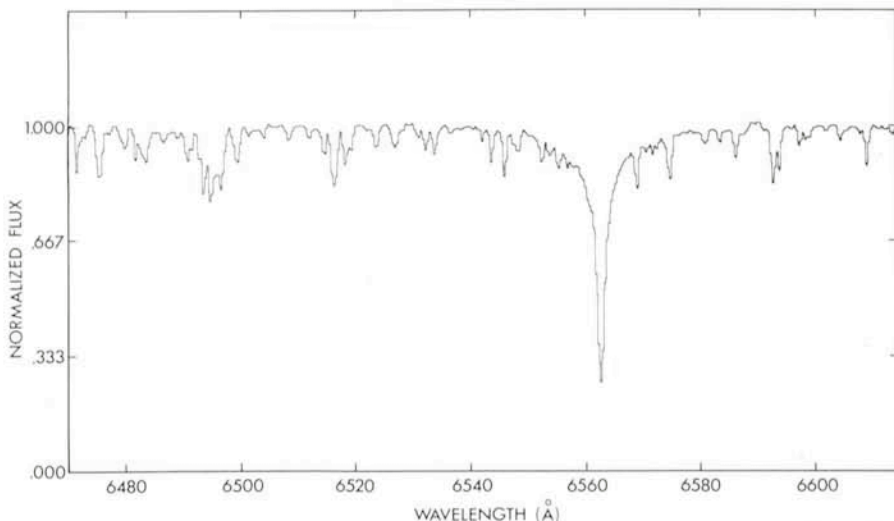


Figure 4: A portion of order 24 extracted from the echellogram of Figure 3 showing the region around H_{α} .

what one expects taking into account the R_s product of this grating (7700 for a 1 arcsec slit), the slit width (0.5 arcsec) and pixel size (0.45 arcsec).

References

Moore, C.E., Minnaert, M.G.J., Houtgast, J.: 1966, *National Bureau of Standards Monograph*, 61.

The Thomson 1024^2 Pixel CCD at the New Technology Telescope

S. D'ODORICO, ESO

Many of the guests who admired on the recent inauguration the impressive images taken with the NTT telescope (see the leading article in this issue of the *Messenger* and Fig. 1) were probably not aware that one of the most important components in the chain that produced those results is a $19 \times 19 \text{ mm}$ silicon device, a 2D detector usually known as a charge-coupled device or in short a CCD, and its associated electronics.

CCDs are nowadays the more intensively used detectors in astronomy because of the convenience of their digital output, the precise geometry of their discrete elements, the good linearity and uniformity, the high quantum efficiency and the low values of the intrinsic sources of noises such as read-out and dark current. At ESO, the six largest telescopes are now equipped with CCD cameras for imaging and spectroscopy and they are used in these modes for the largest fraction of the observing time.

Several industrial companies produce CCDs of interest to astronomical applications: those who currently deliver chips which are in regular use at different telescopes are Thomson CSF and EEV in Europe and Tektronix, Texas In-

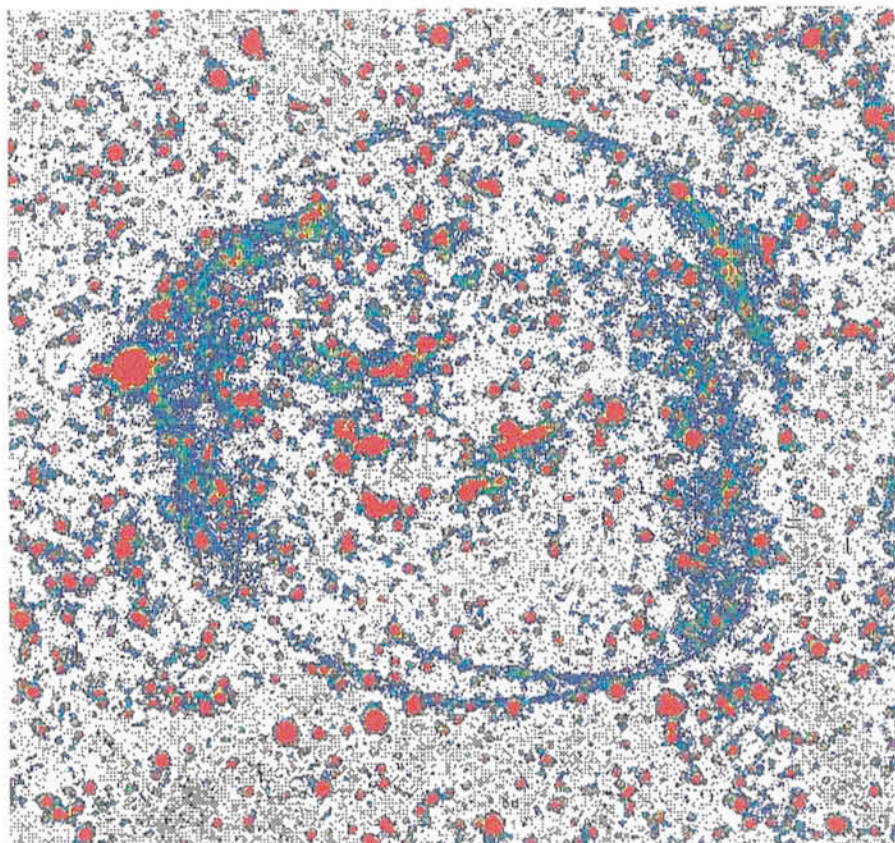


Figure 1: A 30-minute exposure of the Balmer-line dominated supernova remnant 0548-70.4 in the LMC taken at the NTT with EFOSC2 and the Thomson 1024^2 pixel CCD in the light of H_{α} and $[NII]$. In this false-colour reproduction, objects of higher intensity, both stars and nebulae, are shown in red. The field is 2.6×2.6 arcmin with a sampling of 0.152 arcsec/pixel. The low read-out noise of this CCD device ($< 10 e^-/\text{pixel}$) is an important asset for this kind of observations where one wants to detect faint features against a relatively low background.